THE JOURNAL OF BIOLOGICAL CHEMISTRY
Vol. 277, No. 34, Issue of August 23, pp. 31187–31200, 2002

Printed in U.S.A.

Intracellular Assembly of Very Low Density Lipoproteins Containing Apolipoprotein B100 in Rat Hepatoma McA-RH7777 Cells*

Received for publication, January 9, 2002, and in revised form, June 10, 2002
Published, JBC Papers in Press, June 13, 2002, DOI 10.1074/jbc.M200249200

Khai Tran‡, Gro Thorne-Tjomsland§, Cynthia J. DeLong¶, Zheng Cui¶, Jing Shan‡, Lynn Burton‖, James C. Jamieson§, and Zemin Yao‡‡‡**

*From the ‡Lipoprotein & Atherosclerosis Group, University of Ottawa Heart Institute, Ottawa, Ontario K1Y 4W7, Canada, the §Department of Chemistry, University of Manitoba, Winnipeg, Manitoba R3T 2N2, Canada, the ‖Canadian Food Inspection Agency, National Centre for Foreign Animal Disease, Winnipeg, Manitoba R3E 3M4, Canada, the **Department of Pathology & Laboratory Medicine, Department of Biochemistry, Microbiology & Molecular Immunology, University of Ottawa, Ottawa, Ontario K1Y 4W7, Canada, and the ¶Department of Biochemistry, Wake Forest University School of Medicine, Winston-Salem, North Carolina 27157*

Previous studies with McA-RH7777 cells showed a 15–20-min temporal delay in the oleate treatment-induced assembly of very low density lipoproteins (VLDL) after apolipoprotein (apo) B100 translation, suggesting a post-translational process. Here, we determined whether the post-translational assembly of apoB100-VLDL occurred within the endoplasmic reticulum (ER) or in post-ER compartments using biochemical and microscopic techniques. At steady state, apoB100 distributed throughout ER and Golgi, which were fractionated by Nycodenz gradient centrifugation. Pulse-chase experiments showed that it took about 20 min for newly synthesized apoB100 to exit the ER and to accumulate in the *cis*/medial Golgi. At the end of a subsequent 20-min chase, a small fraction of apoB100 accumulated in the distal Golgi, and a large amount of apoB100 was secreted into the medium as VLDL. VLDL was not detected either in the lumen of ER or in that of *cis*/medial Golgi where apoB100 was membrane-associated and sensitive to endoglycosidase H treatment. In contrast, VLDL particles were found in the lumen of the distal Golgi where apoB100 was resistant to endoglycosidase H. Formation of lumenal VLDL almost coincided with the appearance of VLDL in the medium, suggesting that the site of VLDL assembly is proximal to the site of secretion. When microsomal triglyceride transfer protein activity was inactivated after apoB had exited the ER, VLDL formation in the distal Golgi and its subsequent secretion was unaffected. Lipid analysis by tandem mass spectrometry showed that oleate treatment increased the masses of membrane phosphatidylcholine (by 68%) and phosphatidylethanolamine (by 27%) and altered the membrane phospholipid profiles of ER and Golgi. Taken together, these results suggest that VLDL assembly in McA-RH7777 cells takes place in compartments at the distal end of the secretory pathway.

The very low density lipoprotein (VLDL)[1] synthesized in the liver carries various amounts of triacylglycerol (TG) in the neutral lipid core surrounded by phospholipids, cholesterol, and apolipoproteins. Each VLDL particle contains a single copy of apolipoprotein (apo) B100, an extremely hydrophobic and glycosylated polypeptide of ~550 kDa (1). Rat liver secretes VLDL that contains either apoB100 or apoB48 (N-terminal 48% of apoB100). We previously showed that in rat hepatoma McA-RH7777 cells, assembly of apoB48- or apo100-VLDL could be induced by exogenous oleate and was achieved after apoB translation (2). The TG-rich VLDL (*e.g.* $VLDL_1$, $S_f > 100$) that contained ^{35}S-labeled apoB100 was undetectable within the microsomal lumen until 20–40 min after continuous labeling (2). Results from pulse-chase experiments also demonstrated that it took about 35 min (20-min pulse and 15-min chase) for $VLDL_1$ to appear in the lumen of microsomes after apoB synthesis (2). The time spent for $VLDL_1$ assembly is equivalent to that required for newly synthesized apoB100 to traverse through the secretory pathway (3, 4). These results demonstrate that bulk TG is not incorporated into VLDL immediately after apoB100 translation and suggest the existence of post-translational events.

A model that describes the post-translational event and is supported by a good number of experimental evidence is the two-step VLDL assembly model (5–9). According to this model, the newly synthesized apoB100 polypeptides start to recruit, with the assistance of microsomal triglyceride transfer protein (MTP) (2, 10, 11), surface lipids and a small quantity of neutral lipids during and immediately after translation. At this stage, apoB100 polypeptide remains associated with the endoplasmic reticulum (ER) membranes (11, 12), and the resulting lipoprotein particle has buoyant density resembling that of high density lipoproteins (HDL) (13, 14). Normally, these HDL-like particles are not secreted as such. Rather, they combine with

* This work is supported by operating grants from the Canadian Institute of Health Research (to Z. Y.), the Heart and Stroke Foundation of Ontario (to Z. Y.), and the Natural Sciences and Engineering Research Council of Canada (to J. C. J.), National Institute of Health/National Cancer Institute Grant R01CA79670 (to Z. C.), and Signal Transduction and Cellular Function Training Grant CA-09422 (to C. J. D.). The costs of publication of this article were defrayed in part by the payment of page charges. This article must therefore be hereby marked "*advertisement*" in accordance with 18 U.S.C. Section 1734 solely to indicate this fact.

‡‡ Scientist of Canadian Institutes of Health Research. To whom correspondence should be addressed. Tel.: 613-798-5555 (ext. 18711); Fax: 613-761-5281; E-mail: zyao@ottawaheart.ca.

[1] The abbreviations used are: VLDL, very low density lipoprotein; apo, apolipoprotein; Bip, immunoglobulin-binding protein; β-COP, β subunit of coatomer-protein I; COPII, coatomer-protein II; DMEM, Dulbecco's modified Eagle's medium; EEA1, early endosomal antigen 1; Endo H, endoglycosidase H; ER, endoplasmic reticulum; ERGIC, endoplasmic reticulum Golgi intermediate compartment; FBS, fetal bovine serum; Grp, glucose-regulated protein; HDL, high density lipoprotein; Hsp, heat shock protein; IDL, intermediate density lipoprotein; LDL, low density lipoprotein; ManII, α-mannosidase II; MTP, microsomal triglyceride transfer protein; PC, phosphatidylcholine; PE, phosphatidylethanolamine; PNGase F, peptide:*N*-glycosidase F; TEM, transmission electron microscopy; TG, triacylglycerol; TGN, *trans*-Golgi network.

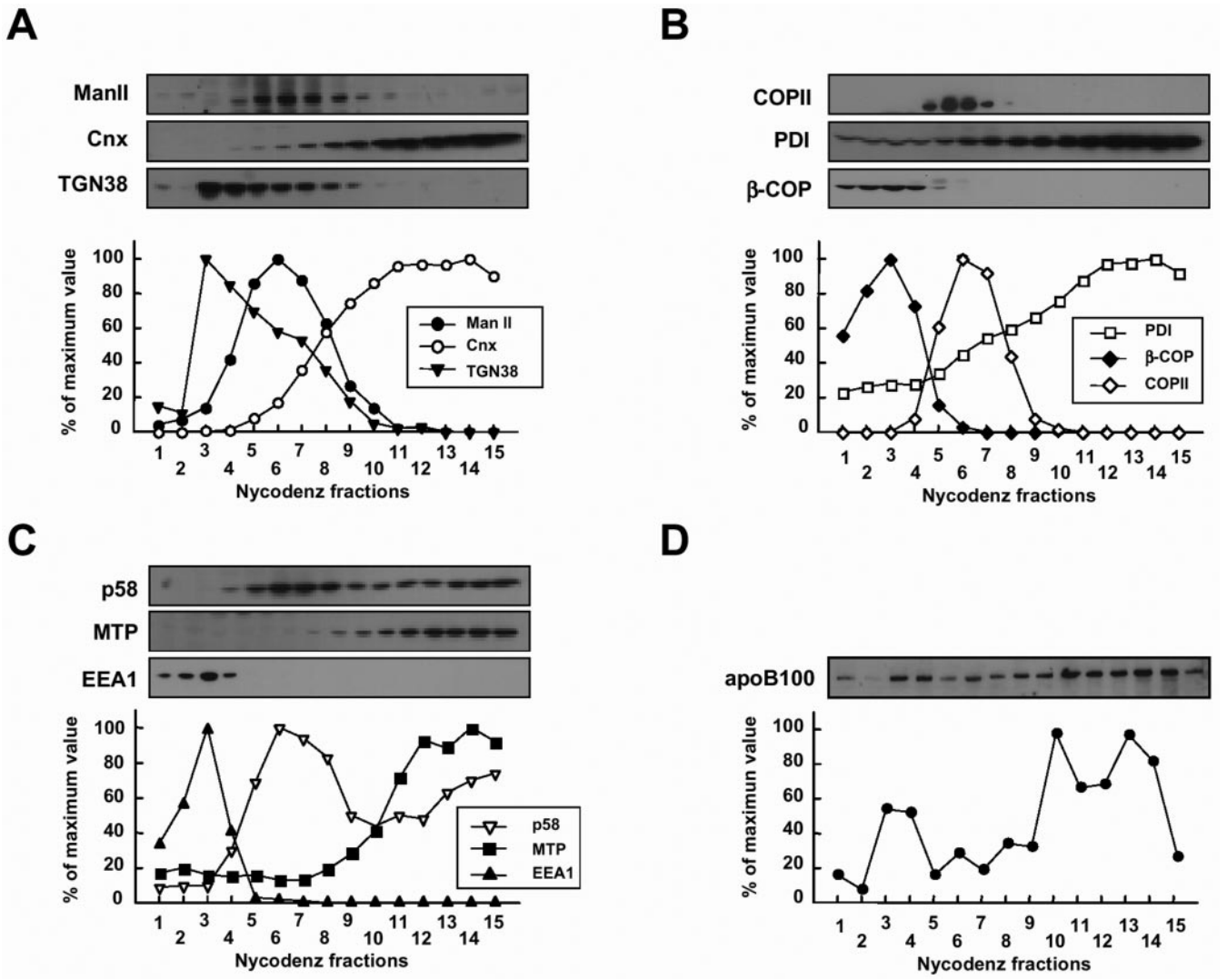

FIG. 1. **Distribution of marker proteins and apoB100 among Nycodenz fractions.** Fractionation of subcellular microsomes by Nycodenz gradient centrifugation was achieved as described under "Experimental Procedures." Proteins of the fractionated samples were resolved by SDS-PAGE (3–15% gel), transferred to nitrocellulose membranes, and immunoblotted with various antibodies. *A*, ManII, calnexin (*Cnx*), and TGN38. *B*, COPII, protein disulfide isomerase, and β-COP. *C*, p58 (a rat analog of human ERGIC53), MTP, and EEA1. *D*, apoB100. The bands on immunoblots were semi-quantified by scanning densitometry, and the intensity was plotted as the percentage of the maximum value in which 100% corresponds to the highest value.

bulk neutral lipids (the second step) to form buoyant low density lipoproteins (LDL), intermediate density lipoproteins (IDL), or VLDL that are detectable in the lumen of microsomes (2, 12). Acquisition of bulk neutral lipids in the second step appears to be independent of the MTP activity (10, 11, 15).

What remains unclear is the subcellular compartments where bulk neutral lipids are incorporated into VLDL containing apoB100. To date, two models have been proposed, and both are supported by experimental evidence. The first model suggests that VLDL assembly takes place in the ER. The "ER assembly" model postulates that the newly synthesized apoB is retained within the rough ER until VLDL, whose size, buoyancy, and lipid composition are indistinguishable from that of secreted VLDL, is fully assembled (16). The resulting ER-derived VLDL is then traversed through the secretory pathway and secreted. The second model theorizes that VLDL assembly occurs in post-ER compartments. This "post-ER assembly" model was suggested by experimental data where the rates of intracellular trafficking between apoB and lipids were compared (4, 17) and the lipid contents of apoB-containing lipoproteins between different subcellular compartments were determined (7, 9). Kinetic analysis provided evidence that the rate of

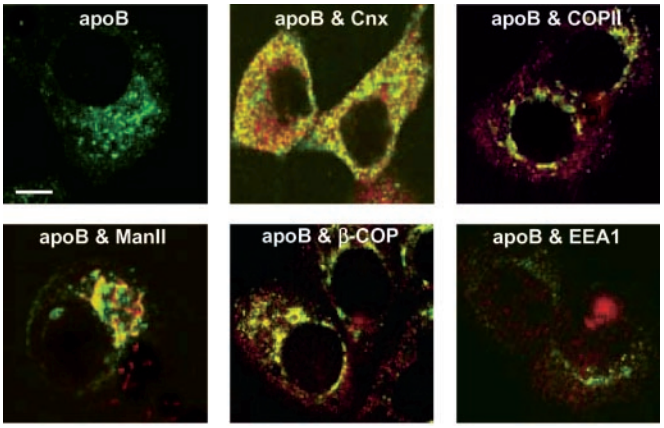

FIG. 2. **Merging confocal images of apoB and markers.** The cells were permeabilized and stained either with anti-human apoB antibody alone or else with anti-apoB antibody plus antibodies against calnexin (*Cnx*), COP-II, ManII, β-COP, or EEA1. The secondary antibodies for apoB were conjugated with Alexa Fluor™ 488 (*green*), and that for marker proteins was conjugated with Alexa Fluor™ 594 (*red*). *Scale bar*, 10 μm for all panels.

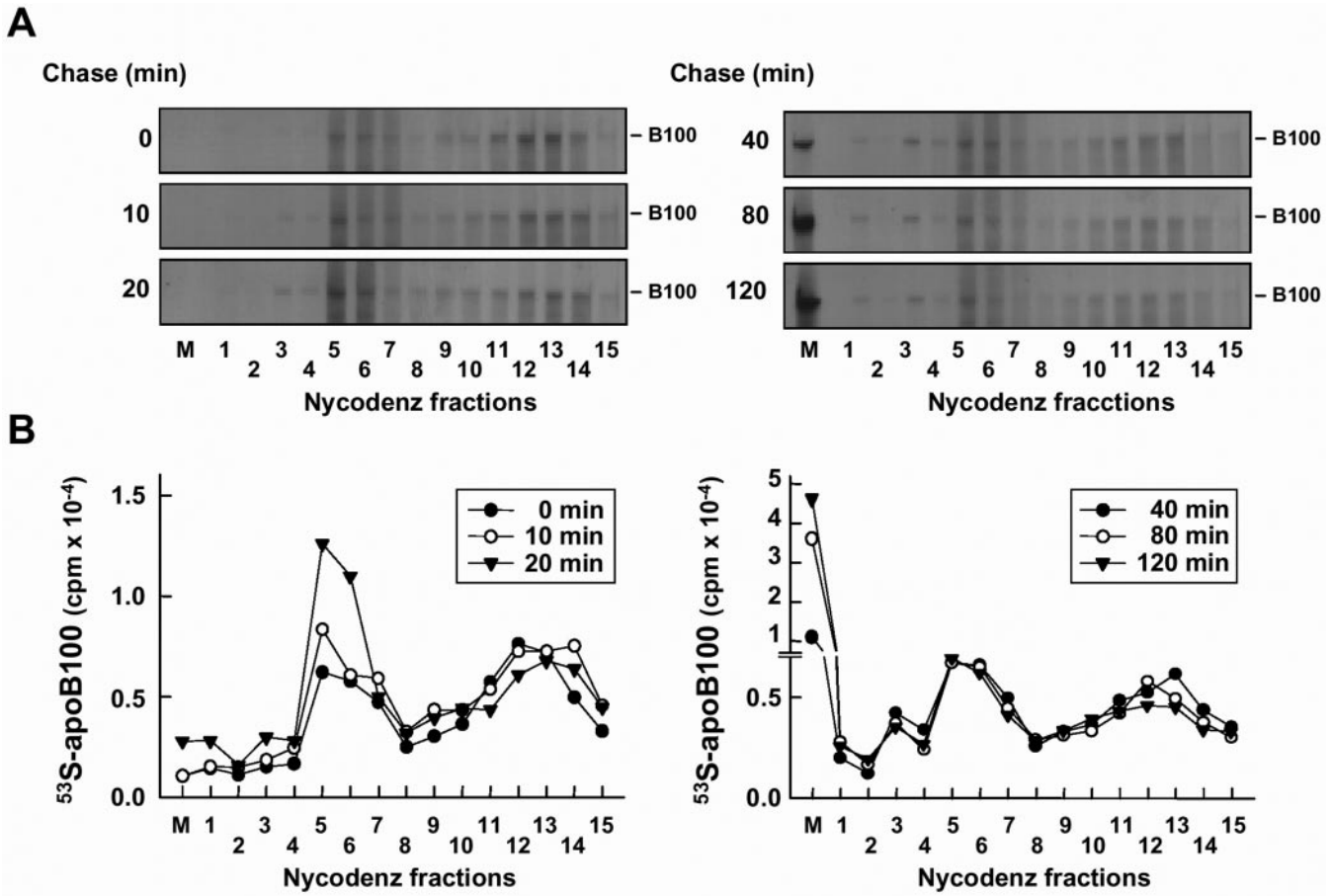

FIG. 3. **Trafficking of radiolabeled apoB100 along the secretory pathway.** The cells were pulse-labeled with [^{35}S]methionine/cysteine for 10 min and chased in the presence of cycloheximide for up to 120 min. At each chase time, medium was collected, and the cells were homogenized followed by Nycodenz fractionation. See "Experimental Procedures" for details. *A*, representative fluorograms of ^{35}S-apoB100 that was secreted into medium (*lanes M*) or associated with the 15 Nycodenz fractions. *B*, quantification of radioactivity associated with ^{35}S-apoB100 by scintillation counting.

TG transit from ER to Golgi was distinct from that of apoB, which ruled in the possibility of a post-ER event (4, 17). Biochemical studies showed the highest amount of lipids associated with apoB in *trans*-Golgi as compared with *cis*-Golgi and rough and smooth ER (7, 9), suggesting a stepwise acquisition of lipids along the secretory pathway (18). Recently, results suggesting post-ER assembly of VLDL containing apoB48 in McA-RH7777 cells have been reported (12). The present study aims to determine the assembly site for VLDL containing apoB100.

EXPERIMENTAL PROCEDURES

Materials—Glycerol [^{14}C]trioleate (57 mCi/mmol), [^{35}S]methionine/cysteine (1000 Ci/mmol), [^{3}H]palmitic acid (52 Ci/mmol), protein A-Sepharose™ CL-4B beads, and horseradish peroxidase-linked anti-mouse or anti-rabbit IgG antibodies were purchased from Amersham Biosciences. Labeled goat anti-mouse (Alexa Fluor™ 488) or anti-rabbit (Alexa Fluor™ 594) IgG antibodies were purchased from Molecular Probes. Endoglycosidase H (Endo H) and peptide:*N*-glycosidase F (PNGase F) were obtained from New England BioLabs. Fibronectin, oleic acid, triacylglycerol, and phospholipid standards were obtained from Sigma and Avanti Polar Lipids. Monoclonal antibody against TGN38 and polyclonal anti-β-COP, -COPII, or -early endosomal antigen 1 (EEA1) were obtained from Affinity Bioreagents. Monoclonal antibody recognizing proteins containing the KDEL motif (Bip, Grp94, and Hsp47) and polyclonal anti-calnexin antiserum were obtained from StressGen. Monoclonal anti-human apoB antibody 1D1 was a gift of R. Milne and Y. Marcel (University of Ottawa Heart Institute). Polyclonal anti-α-mannosidase II (ManII) and anti-MTP antiserum were gifts from M. G. Farquhar (University of San Diego) and C. C. Shoulders (Hammersmith Hospital, London, UK), respectively. Polyclonal antiserum against human LDL was produced in our laboratory. The MTP inhibitor BMS-197636 was a gift of D. Gordon (Bristol-Myers Squibb). Protease inhibitor mixture and chemiluminescent blotting substrate were purchased from Roche Diagnostics. Culture plate inserts (0.4 μm MILLICELL™-CM, 30-mm diameter) were purchased from Millipore.

Cell Culture—Transfected McA-RH7777 cells stably expressing human apoB100 (19) were cultured in Dulbecco's modified Eagle's medium (DMEM) containing 10% fetal bovine serum (FBS), 10% horse serum, and 200 μg/ml G418. During experiments, the cells were kept in DMEM containing 20% FBS plus other reagents as indicated in the figure legends.

Subcellular Fractionation—Two to four 100-mm dishes of cells were harvested in 2 ml of ice-cold homogenizing buffer (10 mM Tris-HCl, pH 7.4, 250 mM sucrose, 5 mM EDTA, and serine/cysteine protease inhibitor mixture) and homogenized by passing 10 times through a ball-bearing homogenizer. Post-nuclear supernatant was obtained by centrifugation (9,500 rpm, 10 min, 4 °C, Sorvall SS-34 rotor) and subjected to fractionation by centrifugation in a Nycodenz gradient as described previously (20, 21). First, a step gradient was created in Beckman SW41 centrifuge tubes by loading (top to bottom) 2.5 ml of 10, 14.66, 19.33, and 24% of Nycodenz solution in saline buffer. The solutions were prepared from 27.6% Nycodenz stock solution and 0.75% NaCl (both in 10 mM Tris-HCl, pH 7.4, 3 mM KCl, 1 mM EDTA, 0.02% NaN_3). The tube was sealed with Parafilm and placed horizontally for 45 min at room temperature followed by centrifugation (37,000 rpm, 4 h, 15 °C, SW41 rotor). Once a nonlinear gradient was formed after centrifugation, 2 ml of the post-nuclear supernatant was layered on top of the gradient and fractionated by centrifugation (37,000 rpm, 1.5 h, 15 °C). After centrifugation, 15 fractions (0.8 ml each) were collected from top of the tube (see Fig. 4*A*, *left three columns*). An aliquot of each fraction (50 μl) was mixed with an equal volume of two-time concentrated protein sample buffer and resolved by SDS-PAGE (3–15% gel). After electrophoresis, the proteins were transferred onto nitrocellulose membranes and probed with anti-

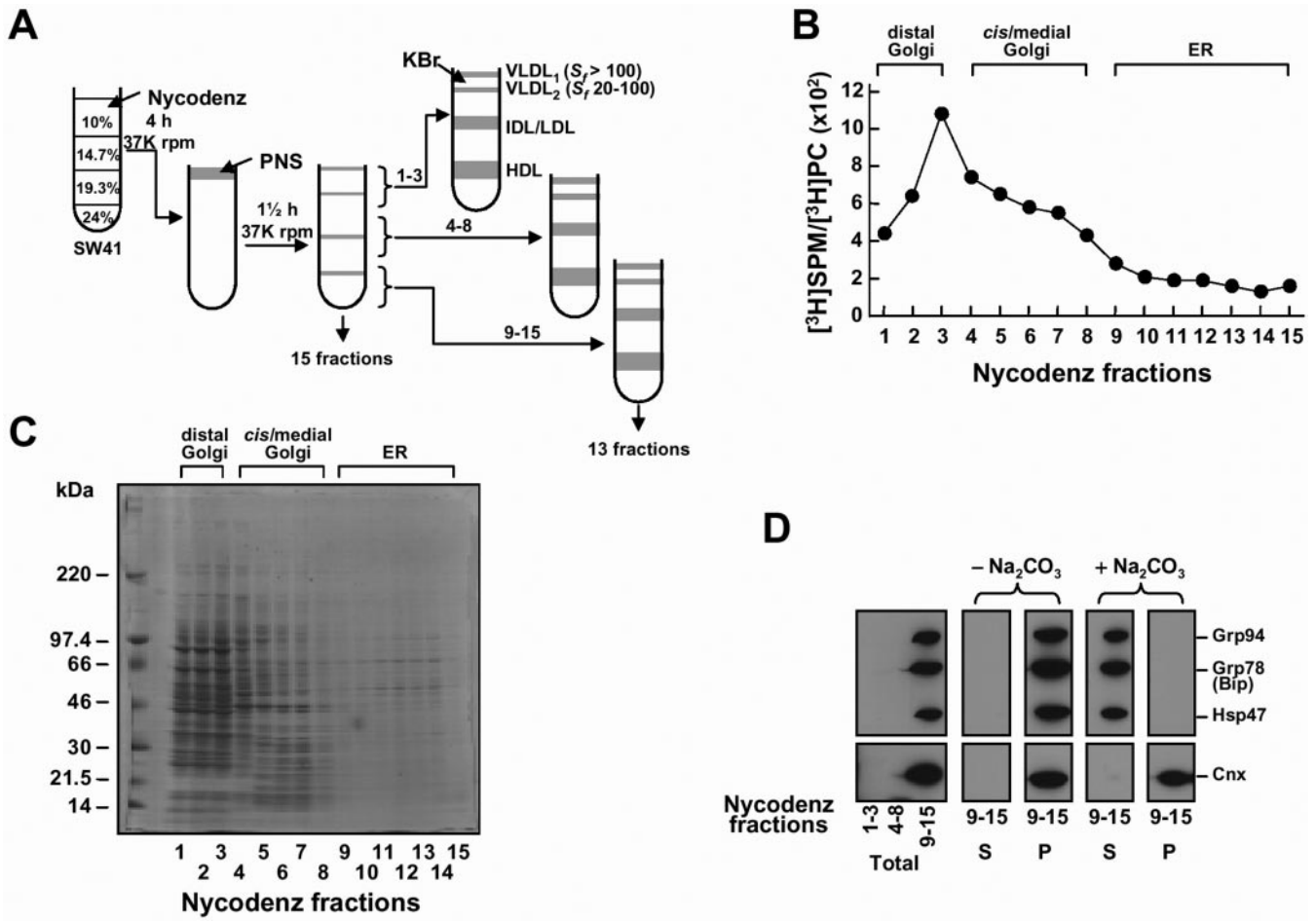

FIG. 4. **Isolation and separation of VLDL from the content of subcellular compartments.** *A*, a protocol used for analyzing buoyancy of lipoproteins containing apoB100 in the fractionated microsomal lumen. *B*, distribution of [^{3}H]palmitate-labeled sphingomyelin among the 15 Nycodenz fractions. The cells were labeled with [^{3}H]palmitic acid (3 μCi) for 4 h prior to subcellular fractionation. The data are presented as the ratio of [^{3}H]sphingomyelin/[^{3}H]PC. *C*, protein profile of the 15 Nycodenz fractions. The gel was stained with Coomassie Blue. *D*, pooled Nycodenz fractions (1–3, 4–8, and 9–15) were mixed with or without equal volume of 0.2 M Na_2CO_3, pH 12.4, for 30 min and subjected to ultracentrifugation to separate membranes (as pellet, *P*) from lumenal content (as supernatant, *S*). The proteins were resolved by SDS-PAGE and blotted using anti-calnexin (*Cnx*) antibody or anti-KDEL antibody to visualize Grp94, Bip, and Hsp47.

bodies specific for marker proteins of various subcellular compartments.

Immunocytochemistry—The cells were plated on coverslips for 24 h, fixed with 3% paraformaldehyde in phosphate-buffered saline for 20 min, and permeabilized with 0.1% Triton X-100 (in phosphate-buffered saline) for 3 min. The cells were incubated with 10% FBS (in phosphate-buffered saline) for 20 min prior to probing with antibodies. Monoclonal antibody 1D1 (1:1000 dilution) was used to probe the recombinant human apoB (1 h) followed by incubation with goat anti-mouse IgG conjugated with Alexa Fluor™ 488 (1:200 dilution) as a secondary antibody (1 h). Subcellular compartments were probed with antibodies against calnexin (1:500 dilution) for ER, COPII (1:150 dilution) for ER-to-Golgi anterograde vesicles, ManII (1:500 dilution) for *cis*/medial Golgi, β-COP (1:100 dilution) for Golgi anterograde/retrograde vesicles, and EEA1 (1:100 dilution) for endosomes. The secondary antibody was Alexa Fluor™ 594 conjugated with anti-rabbit IgG (1:200). All incubations and washes were performed at room temperature. After immunostaining, the coverslips were mounted onto a glass slide using SlowFade AntiFade kits (Molecular Probes). The images were captured by a MRC-1024 laser scanning confocal imaging system.

Pulse-Chase Experiments—In pulse-chase experiments where lumenal apoB100 particles of different subcellular fractions were determined, the cells in two 100-mm dishes were labeled with [^{35}S]methionine/cysteine (200 μCi/ml in 3 ml of methionine- and cysteine-free DMEM containing 20% FBS and 0.4 mM oleate) for 20 min. The cells were then incubated with chase medium (DMEM containing 20% FBS and 0.4 mM oleate) for 15, 30, and 45 min. At the end of each chase time, the medium was collected and subjected to cumulative rate flotation centrifugation (2) to resolve apoB100-$VLDL_1$ ($S_f > 100$) and apoB100-$VLDL_2$ (S_f 20–100) from other lipoproteins (*i.e.* IDL, LDL, and HDL). The ^{35}S-apoB100 in each fraction was recovered by immunoprecipitation using polyclonal antiserum raised against human LDL as described previously (22). Also, at the end of each chase time, the radiolabeled cells were harvested in 2 ml of ice-cold homogenization buffer, mixed with two 100-mm dishes of unlabeled cells, and subjected to subcellular fractionation and carbonate treatment as described below.

In experiments where transit of newly synthesized apoB100 along the secretory pathway was determined, the cells were pulse-labeled for 10 min, washed, and incubated with chase medium containing 10 μM cycloheximide for 10, 20, 40, 80, and 120 min. The medium and cell samples were processed at the end of chase time as described above, except that the one dish of labeled cells was mixed with one dish of unlabeled cells prior to subcellular fractionation. In experiments where intracellular distribution of membrane- and lumen-associated apoB100 was determined, the cells were pulse-labeled for 20 min and incubated with chase medium for 0, 15, 30, and 45 min. apoB100 associated with membrane and lumenal content was isolated and analyzed as described below.

In experiments where MTP was inactivated by BMS-197636, two protocols were used. In the first protocol, MTP activity was inhibited prior to apoB synthesis. To do this, cells were incubated with 0.2 μM BMS-197636 for 30 min, pulse-labeled with 200 μCi/ml [^{35}S]methionine/cysteine for 20 min, and chased first for 15 min and second with fresh medium for additional 30 min. Oleate (0.4 mM) and BMS-197636 (0.2 μM) were present throughout pulse and chase. In the second protocol, MTP activity was inhibited after apoB had exited the ER. To achieve this, the MTP inhibitor was added to the medium during the second chase (30 min).

Analysis of apoB100 Associated with Membranes and Lumenal Contents of Microsomes—Each Nycodenz fraction was added with an equal

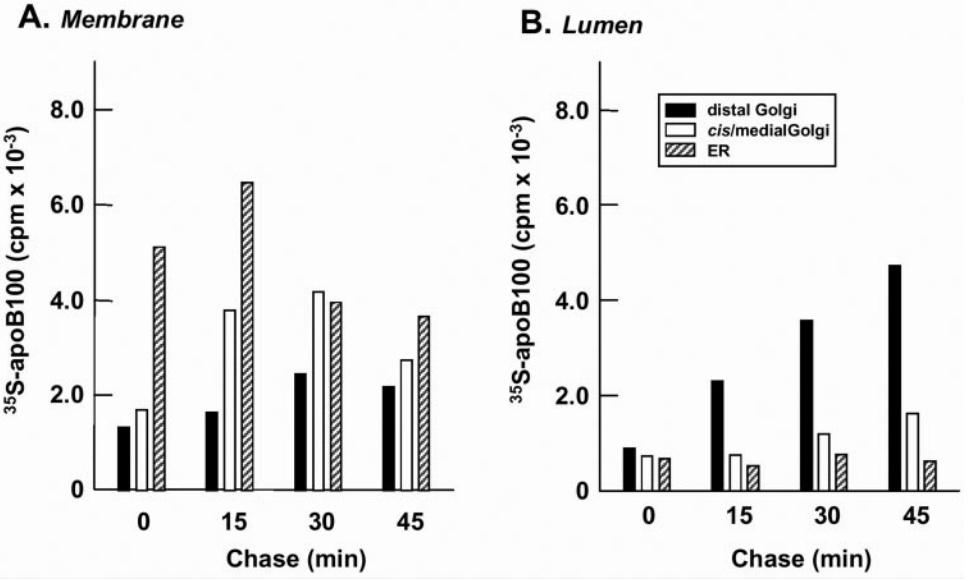

FIG. 5. **Intracellular distribution of membrane and lumenal ^{35}S-apoB100 during chase.** The cells were pulse-labeled with [^{35}S]methionine/cysteine for 20 min and chased for the indicated times. The cells were homogenized followed by Nycodenz fractionation. ^{35}S-apoB100 in the membrane (*A*) and lumen (*B*) of pooled microsomal fractions (fractions 1–3, 4–8, and 9–15) was analyzed by immunoprecipitation and SDS-PAGE as described under "Experimental Procedures."

volume of 0.2 M Na_2CO_3, pH 12.4 (to reach a final concentration of 0.1 M and pH 11.3) and gently mixed for 30 min at room temperature. The membranes were pelleted by centrifugation (100,000 rpm, 15 °C, 16 min, TLA 100.4 rotor) and resuspended in 0.2 ml of lysis buffer (1% SDS, 1% Triton X-100, 1% sodium deoxycholate, 0.5 mM EDTA, 15 mM NaCl, 1 mM dithiothreitol, 0.15% phenylmethylsulfonyl fluoride, 50 mM Tris-HCl, pH 8.0). The mixture was diluted to 0.2% SDS, and apoB was recovered by immunoprecipitation. For lumenal apoB100, the 15 Nycodenz fractions were pooled into three groups: fractions 1–3, 4–8, and 9–15 (see Fig. 4*A*, *right three columns*). Each group was dialyzed against 250 mM sucrose in 10 mM Tris-HCl, pH 7.4, for 2 h at room temperature to remove Nycodenz and mixed with an equal volume of 0.2 M Na_2CO_3, pH 12.4, as described above. In some experiments, lumenal apoB100 was released by carbonate treatment in the presence of 0.025% sodium deoxycholate and 1.2 M potassium chloride as described (11, 22). The lumenal content of the carbonate-treated microsomes was separated from membranes by centrifugation (100,000 rpm, 15 °C, 16 min, TLA 100.4 rotor) and subjected to cumulative rate flotation centrifugation (2).

Endo H and PNGase F Digestion—Immunoprecipitated apoB100 from ^{35}S-labeled or unlabeled samples was eluted from protein A-Sepharose beads by mixing with 90 μl of denaturing buffer (50 mM Tris-HCl, pH 6.8, 0.5% SDS, 1% 2-mercaptoethanol). The mixture was heated at 95 °C for 10 min, and an aliquot (30 μl) was mixed with either 3 μl of 0.5 M sodium citrate, pH 5.5, for Endo H (500 units) digestion or else 3 μl of 0.5 M sodium phosphate, pH 7.5, for PNGase F (500 units) digestion (both 4 h at 37 °C). The apoB100 and ^{35}S-apoB100 were analyzed by PAGE/immunoblot and PAGE/fluorography, respectively. The membrane-associated apoB100, because of its abundance, was detected by immunoblotting, and the lumenal apoB100 was detected by radiolabeling (see figure legends for details).

Tandem Mass Spectrometry—The cells were kept in DMEM (20% FBS ± 0.4 mM oleate) for 16 h and reincubated with fresh medium (20% FBS ± 0.4 mM oleate) for additional 2 h. The membrane and lumen samples of Nycodenz fractions 1–3, 4–8, and 9–15 were derived from cells pooled from eight 100-mm dishes. The conditioned media were subjected to cumulative rate flotation centrifugation (2). The lipids were extracted from the samples with chloroform/methanol/acetic acid/saturated NaCl/H_2O (4:2:0.1:1:2, by volume) in the presence of 230 pmol of dimirystoyl (14:0-14:0) PC and 110 pmol of dipalmitoyl (16:0-16:0) PE as internal standards. Aliquots of lipid extracts were applied to tandem mass spectrometry, and the molecular species (*i.e.* fatty acid composition) of PC and PE was determined by daughter ion analysis in the negative ion mode as described previously (22, 23). The integrated area under the peak or peak height of each molecular species was quantified by comparing with that of internal standards.

Transmission Electron Microscopy—The cells were cultured in normal culture medium on MILLICELL™-CM insert membranes precoated with fibronectin for 20 h and incubated for additional 2 h with fresh DMEM containing 20% FBS and 0.4 mM oleate. After rinsing with serum-free DMEM three times (5 min/rinse), the cells were prefixed for 1 h at room temperature with 2% glutaraldehyde in 0.1 M sodium cacodylate buffer (pH 7.4) containing 0.05% $CaCl_2$ and post-fixed for 1 h at 4 °C with 1% OsO_4, 1.5% potassium ferrocyanide (24). After rinsing with cacodylate buffer, the cells attached to the insert membranes were dehydrated in a series of ethanol and embedded in Epon in a Fisher metal foil pan (polymerization at 68 °C). Epon disks were cut into ~2.5 × 2.5 × 1-mm^3 pieces, which were mounted on Epon blocks with insert membranes oriented parallel to the cutting surface. Sections of silver-gold interference colors (60–150 nm) were cut on a Leica ultracut UCT microtome and placed on Formvar-coated, slotted copper grids. The grids were stained for 20 min with uranyl acetate and for 10 min with lead citrate and viewed at 75 kV in a Hitachi H-7000 transmission electron microscope. The diameters of lipoproteins were measured in 94 Golgi stacks from over 50 cells. Photographs were taken at negative magnification of 30,000 times, with positives magnified an additional 2.7–2.8 times. Included were all Golgi stacks with more than one lipoprotein/stack and definable *cis-trans* polarity by the presence of at least two of the following characteristics: 1) microtubules oriented parallel to *cis*-Golgi; 2) large perforations in *cis*-element; 3) clathrin-coated buds and vesicles on *trans*-Golgi; and 4) lipoprotein-filled secretory granules near *trans*-Golgi. Only particles definable along their entire circumference were included. For oval-shaped particles, the long diameter was measured.

Other Assays—The TG transfer activity of MTP was determined according to a published method (25) with modifications (2). Briefly, after incubation with 0–0.5 μM MTP inhibitor BMS-197636 (in the presence of 0.4 mM oleate) for 30 min, the cells were homogenized using a ball-bearing homogenizer and sonicated twice for 30 s. The whole cell lysate was used in the glycerol [^{14}C]trioleate transfer assay. The protein was determined using the BCA protein assay kit (Pierce).

RESULTS

Subcellular Distribution of apoB100—Subcellular compartments were fractionated using a Nycodenz gradient, and each fraction was probed with antibodies specific to marker proteins by immunoblot analysis (Fig. 1, *A–C*). Three distinct subcellular compartments, namely ER, *cis*/medial Golgi, and distal Golgi, were separated. Fractions 9–15 were designated ER by their possessing of calnexin, MTP, protein disulfide isomerase, Grp78 (Bip), Grp94, and Hsp47 (see Fig. 4*D*). Fractions 4–8 were designated *cis*/medial Golgi because they contained ManII and COPII (marker for ER-to-Golgi anterograde vesicles). The intermediate compartment between ER and Golgi

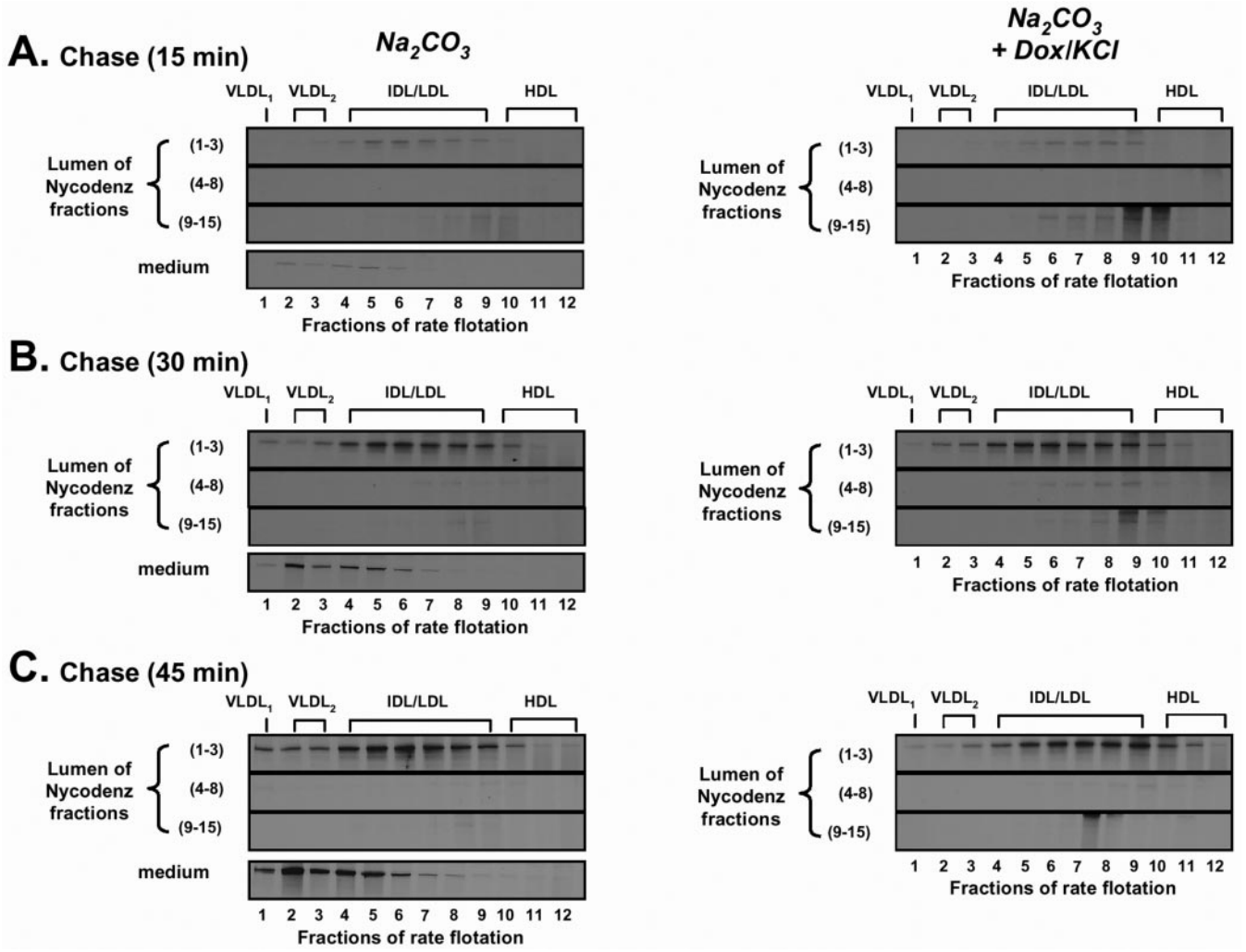

FIG. 6. **Lumenal ^{35}S-apoB100 containing lipoproteins in subcellular compartments during chase.** The cells were pulse-labeled with [^{35}S]methionine/cysteine for 20 min and chased for 15 min (*A*), 30 min (*B*), and 45 min (*C*). At the indicated chase time, the medium was collected and subjected to cumulative rate flotation centrifugation, whereas the cells were homogenized followed by Nycodenz fractionation. The pooled microsomal fractions (fractions 1–3, 4–8, and 9–15) were treated with sodium carbonate in the absence (*left panels*) or presence (*right panels*) of sodium deoxycholate and potassium chloride (*Dox/KCl*). The buoyancy of lipoproteins containing ^{35}S-apoB100 was analyzed by cumulative rate flotation centrifugation. See "Experimental Procedures" for details.

marker p58 (a rat analog of human ERGIC53) had a bimodal distribution with two peaks at ER (fraction 15) and *cis*/medial Golgi (fraction 6), respectively. Fractions 1–3 represent a mix of *trans*-Golgi network, early endosome, and Golgi-derived retrograde/anterograde vesicles by appearance of TGN38, EEA1, and β-COP. At steady state, apoB100 distributed throughout the entire secretory pathway (Fig. 1*D*). Merging confocal images of immunocytochemistry confirmed co-localization of apoB (*green color*) with ER (calnexin), *cis*/medial Golgi (COPII and ManII), and distal Golgi (β-COP) markers (*red color*) (Fig. 2). However, apoB100 did not co-localize with the endosomal marker EEA1.

Intracellular Trafficking of apoB100—Intracellular trafficking of apoB100 was monitored by pulse-chase experiments (cycloheximide was included in chase medium to prevent protein elongation) in conjunction with subcellular fractionation. At the end of the 10-min pulse, the majority of ^{35}S-apoB100 was located in the ER, whereas a small portion appeared in *cis*/medial Golgi (Fig. 3*A*, *0 min chase*). The presence of apoB100 in *cis*/medial Golgi after 10 min of labeling was not unexpected because translation was unsynchronized in these cells. Accumulation of ^{35}S-apoB100 in *cis*/medial Golgi became obvious at 10 min and peaked at 20 min during chase. At the end of a 40-min chase, ^{35}S-apoB100 appeared in distal Golgi (fraction 3), and secretion of ^{35}S-apoB100 into the medium was detectable. Prolonged chase (*i.e.* 80 and 120 min) resulted in further accumulation of ^{35}S-apoB100 in the medium but did not result in accumulation of ^{35}S-apoB100 in distal Golgi. These results suggest that newly synthesized apoB100 traverses at a relatively slow rate through *cis*/medial Golgi but transits rather rapidly through distal Golgi.

VLDL in Distal Golgi Lumen—To determine which Nycodenz fraction(s) contained VLDL, we analyzed the buoyancy of lipoproteins containing apoB100 within the lumenal of pooled ER (fractions 9–15), *cis*/medial Golgi (fractions 4–8), and distal Golgi (fractions 1–3) microsomes (Fig. 4*A*). In addition to marker distributions shown in Fig. 1, pooling of these microsomal membranes was justified by the distribution of [^{3}H]palmitate-labeled sphingomyelin (a Golgi-synthesized lipid) (Fig. 4*B*) and by overall protein patterns of the Nycodenz fractions (Fig. 4*C*). Separation of lumen from membrane after sodium carbonate treatment was complete, as evidenced by the appearance of Grp94, Bip, and Hsp47 in the supernatant and that of calnexin in the pellet of the ER microsomes (Fig. 4*D*, *panels* marked + Na_2CO_3) after centrifugation.

Using the protocol depicted in Fig. 4*A*, we analyzed the kinetics of apoB100-VLDL assembly and secretion at various chase times. At the beginning of chase, the majority of ^{35}S-

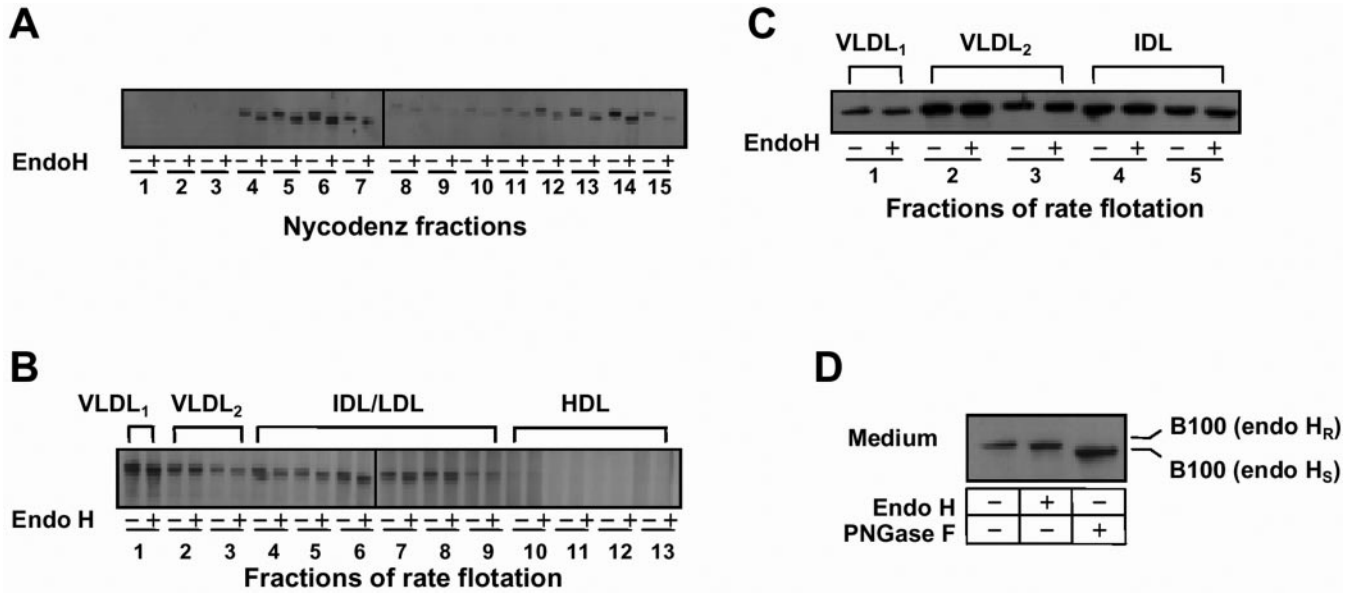

FIG. 7. **Membrane-associated apoB100 is sensitive to Endo H.** *A*, cells were incubated with 0.4 mM oleate for 2 h and subjected to Nycodenz fractionation. The nonradiolabeled apoB100 was immunoprecipitated from the membranes of 15 Nycodenz fractions, treated with (+) or without (−) Endo H, and analyzed by SDS-PAGE/immunoblotting. *B*, cells were pulse-labeled with [^{35}S]methionine/cysteine for 20 min, chased for 45 min, and subjected Nycodenz fractionation. The fractions representing distal Golgi were pooled (fractions 1–3), and the lumenal content was subjected to cumulative rate flotation centrifugation. The ^{35}S-apoB100 was immunoprecipitated from each lipoprotein fractions and treated with or without Endo H prior to SDS-PAGE/fluorography analysis. *C*, immunoblots of medium apoB100 secreted as $VLDL_1$, $VLDL_2$, or IDL. The samples were treated with or without Endo H as described above. *D*, immunoblots of apoB100 associated with total medium. Treatment with PNGase F was used to verify the complex glycosylation status of apoB100.

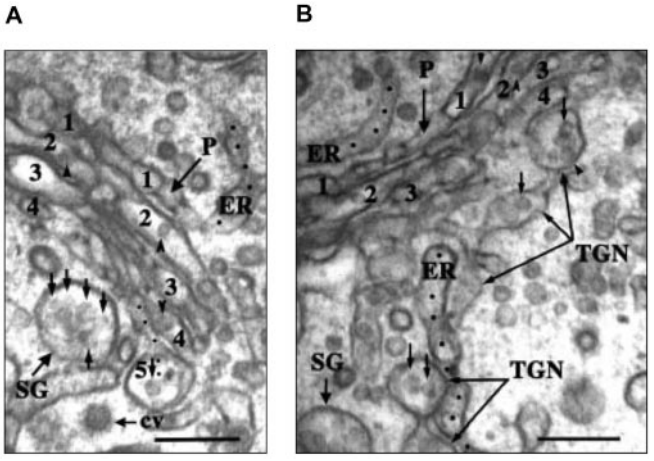

FIG. 8. **Transmission electron microscopy of lipoprotein particles within the Golgi region.** The cells were processed and visualized for TEM as described under "Experimental Procedures." Lipoprotein particles were undetectable in the ER (*stippled lines*), on either the *cis*- or *trans*-sides of the Golgi stack. Golgi saccules from *cis* to *trans* are labeled *1–5* (*panels A* and *B*). The *cis* to *trans* polarity of Golgi stacks was assigned by the presence of large perforations (*P*) in the *cis*-element (saccule 1) and by secretory granules (*SG*) and the coated vesicle (*cv*; *panel A*) near the *trans*-Golgi. Lipoprotein particles in the *cis*-Golgi tend to be smaller than in the *trans*-Golgi, but intrasaccule variation in lipoprotein diameter can be imaged. In saccules 1, 2, and 4, lipoprotein particles show membrane association (*arrowheads*). In saccule 5 (*A*), TGN (*B*), and SGs, lipoproteins are mainly lumenal (*arrows*) with occasional membrane association (*arrowhead* in *B*). *Scale bars*, 200 nm.

apoB100 was associated with the membrane of ER (Fig. 5*A*). The amount of ^{35}S-apoB100 radioactivity in the ER membranes decreased during chase (between 15 and 45 min), and the lost radioactivity could be quantitatively recovered in *cis*/medial Golgi membranes (Fig. 5*A*) and in distal Golgi lumen (Fig. 5*B*). Thus, degradation of newly synthesized ^{35}S-apoB100 was insignificant within this time frame. Trace amount of ^{35}S-apoB100 in the form of VLDL could be detected in the medium at 15-min chase, although apoB100-VLDL was not detectable in the lumen of distal Golgi at this time (Fig. 6*A*, *left panel*). By the time of 30- and 45-min chase, the amount of ^{35}S-apoB100 associated with VLDL increased in the distal Golgi as well as in the medium (Figs. 5*B* and 6, *B* and *C*, *left panels*). Notably, the amount of ^{35}S-apoB100 associated with VLDL in the lumen was 10–20-fold lower than that secreted in the medium at all chase times, indicating rapid release of VLDL once they are assembled. During the entire chase, only trace amounts of ^{35}S-apoB100 were detectable in the lumen of ER or *cis*/medial Golgi (Fig. 5*B*), even though a considerable amount of apoB100 was present in these compartments (Figs. 1*D*, 3, and 5*A*). The low abundance of ^{35}S-apoB100 in the ER lumen was unlikely due to incomplete treatment by sodium carbonate, because the ER residence proteins Grp94, Bip, and Hsp47 were effectively released into the lumen under the same conditions (Fig. 4*D*).

The near absence of ^{35}S-apoB100 in the ER or *cis*/medial Golgi lumen suggested that apoB100 in the early secretory compartments was mainly membrane-bound and could not readily be removed by carbonate treatment. We attempted to remove the membrane-associated apoB100 from fractionated microsomes with sodium carbonate plus sodium deoxycholate and potassium chloride (11, 22). Under these conditions, the amount of ^{35}S-apoB100 particles associated with lipoproteins of high buoyant density was increased in the lumen of ER, *cis*/medial Golgi, and distal Golgi (Fig. 6, *A–C*, compare *right panels* and *left panels*). However, no increase in ^{35}S-apoB100 was found in fractions containing VLDL. These data suggest that the membrane-associated apoB100 is poorly lipidated within the early secretory compartments.

To ascertain that the membrane-bound apoB100 was indeed associated with microsomes of early secretory pathway, we determined the glycosylation status of apoB100 by Endo H digestion. In cells where lipogenesis was maximized by exogenous oleate, membrane-bound apoB100 in ER and *cis*/medial Golgi was Endo H-sensitive (Fig. 7*A*). However, once apoB100 reached distal Golgi, it became associated with lipoproteins of

TABLE I
Lipoprotein diameter changes with transit through consecutive Golgi saccules, the TGN, and secretory granules
TEM processing of cells and measurements of lipoprotein diameter were performed as described "Experimental Procedures." The diameters of a total of 1025 lipoprotein particles were measured.

	Golgi saccules						TGN	SG
	1	2	3	4	5	6		
Average diameter (nm)	33 ± 11 (n = 98)	36 ± 12 (n = 112)	41 ± 15 (n = 112)	44 ± 19 (n = 138)	41 ± 16 (n = 101)	46 ± 19 (n = 95)	42 ± 16 (n = 233)	40 ± 11 (n = 136)
Range (nm)	12–86	19–86	12–123	18–148	19–123	19–148	12–123	24–80
Median (nm)	31	31	37	39	37	43	37	37

varied buoyancy and was Endo H-resistant (Fig. 7*B*). As was the case for that in distal Golgi, apoB100 secreted in the form of $VLDL_1$, $VLDL_2$, and IDL was also Endo H-resistant (Fig. 7*C*). In a control experiment, the presence of complex oligosaccharides on the Endo H-resistant apoB100 molecules was verified by digestion with PNGase F (Fig. 7*D*). These results demonstrate that the formation of lipoproteins containing apoB100 coincided with the gaining Endo H-resistance of apoB100. The presence of $VLDL_1$ containing ^{35}S-apoB100 within distal Golgi lumen but not ER or *cis*/medial Golgi lumen was similarly observed in pulse-chase experiments using cultured primary rat hepatocytes (data not shown).

Transmission Electron Microscopy Analysis of Subcellular Distribution of Lipoprotein Particles—To ascertain that VLDL particles were not formed within the ER, we analyzed the distribution of lipoproteins within the secretory pathway of McA-RH7777 cells by single and serial section transmission electron microscopy (TEM). The apparent absence of lipoprotein particles in Golgi-associated ER was noted. However, electron-dense particles were found in dilations of Golgi saccules (from *cis-trans*), in the TGN, and in secretory granules (Fig. 8). These electron-dense particles are mainly apolipoprotein-containing particles as demonstrated previously (26) but may include lipid droplets devoid of apolipoproteins. The Golgi stacks sampled contained on average 11 particles/sectioned stack, and about 40% of the stacks contained less than 5 particles/stack. It was noted that lipoproteins in the *cis*-Golgi frequently were membrane-associated, whereas those in the *trans*-Golgi, TGN, and secretory granules were not (Fig. 8).

The average diameter of pooled lipoproteins from all Golgi saccules (saccules 1–6 in Table I) was 40 ± 17 nm (n = 656). An incremental increase in the average diameter of particles occurred in each saccule (except for saccule 5); between the *cis*-most (saccule 1) and the *trans*-most (saccule 6) elements, the increase was 1.4-fold (Table I). In post-Golgi compartments, the average lipoprotein diameter decreased. Thus, the average diameter of particles in the TGN was 9% smaller than that in saccule 6, and a further 5% decrease in particle size occurred between the TGN and secretory granules. The increase in lipoprotein size from *cis* to *trans* saccules was also evident when data were presented in the form of histograms (Fig. 9). Five species of particles with increasing size denoted as *1 to *5 were identified for saccules 1–3 (Fig. 9*A*) and for saccules 4–6 plus TGN (Fig. 9*B*). The incidence of species *1, *2, *3, and *4–5 (relative to total lipoprotein particles between 10–75 nm) was 6.2, 66.5, 18.8, and 8.5%, respectively, in the *cis* elements (saccules 1–3) and 4.4, 52, 29.6, and 14%, respectively, in the *trans* elements (saccules 4–6 plus TGN). Thus, between *cis* and *trans* saccules, a shift occurred from two smaller diameter species (*1 and *2) toward three larger diameter species (*3, *4, and *5).

Assembly of VLDL after apoB Exits ER Requires No MTP Activity—Knowing that VLDL assembly possibly occurred in post-ER compartments, we then inquired whether the MTP activity is required at this stage. Because MTP was found predominantly in the ER (Fig. 1*C*), we hypothesized that the post-ER VLDL assembly required no MTP activity. To test this hypothesis, we designed two pulse-chase protocols by which the MTP was inactivated either before or after metabolic labeling of apoB100 under conditions where lipogenesis was maximized by exogenous oleate. When the MTP inhibitor BMS-197636 was added to the medium 30 min before the pulse labeling, secretion of ^{35}S-apoB as VLDL during chase was virtually abolished as compared with the control (*i.e.* no MTP inhibition) (Fig. 10*A*, compare *top* and *middle panels*). Inactivation of MTP before metabolic labeling also blocked formation of VLDL containing

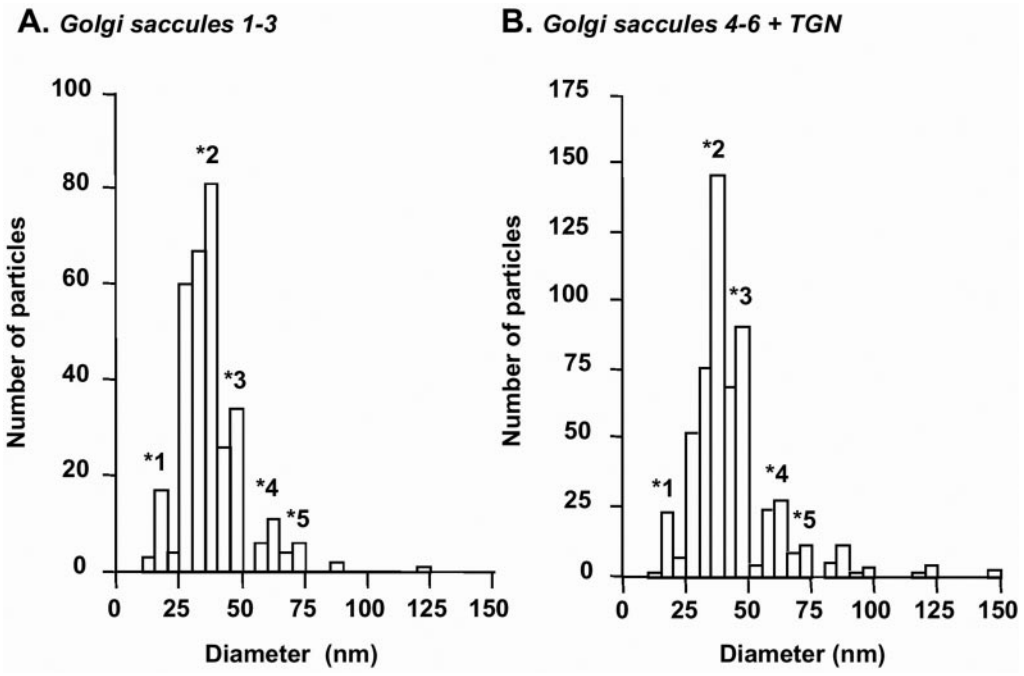

FIG. 9. **Comparison of the size distribution of lipoprotein particles between *cis*- and *trans*-Golgi.** Histograms of pooled lipoprotein diameter data for saccules 1–3 (*A*) and saccules 4–6 plus TGN (*B*) revealed five species of particles of increasing size denoted as **1* to **5*. Each species was represented by multiple columns, where the highest column corresponds to the diameter of that species at its equator, whereas the stepwise decreasing columns to the *left* likely represent cross-sections of that species away from its equator.

^{35}S-apoB100 in the distal Golgi lumen (Fig. 10*B*, compare *top* and *middle panels*). However, if MTP was inactivated 15 min after chase commenced, secretion of ^{35}S-apoB100 as VLDL (Fig. 10*A*, *bottom panel*) or the assembly of VLDL-containing ^{35}S-apoB100 in distal Golgi lumen (Fig. 10*B*, *bottom panel*) was unaffected during the subsequent 30-min chase, even though the MTP activity was decreased to 20% of the normal level (Fig. 10*C*). This latter time frame of MTP inactivation was designed based on the observation that VLDL was not detectable in the lumen after 15 min of chase but appeared after 30 and 45 min of chase (Fig. 6). At the dose of BMS-197636 used in these experiments, the translation of apoB100 was not affected (Fig. 10*D*). The results of these experiments are evidence that once apoB100 has exited ER, the exogenous oleate-induced VLDL assembly requires no MTP activity and therefore is insensitive to MTP inhibition.

Molecular Species of Phospholipids in Subcellular Compartments—In McA-RH7777 cells, molecular species of phospholipids are regulated by deacylation and reacylation processes that are stimulated when exogenous oleate is added to the medium to induce VLDL assembly and secretion (22). We hypothesized that oleate treatment might produce a unique membrane milieu composed of phospholipids with molecular species especially suitable for VLDL assembly. As a first attempt to test this hypothesis, we determined the effect of oleate treatment on molecular species of membrane PC and PE in the secretory compartments. As shown in Fig. 11 (*A* and *B*), although oleate treatment resulted in increase in PC (by 68%) and PE (by 27%) mass in the membranes of total microsomes, this increase did not occur uniformly in all subcellular compartments. Thus, the increase in PC mass was observed in the ER (by 139%) and distal Golgi (by 127%) membranes, whereas the PC mass in the *cis*/medial Golgi membranes was decreased. Likewise, the increase in PE mass was observed only in the ER membrane (by 186%), whereas the PE mass in both distal and *cis*/medial Golgi membranes was decreased (Fig. 11, *A* and *B*, *bottom panels*).

As summarized in Table II, marked molecular species remodeling occurred to membrane PC and PE by oleate treatment. Although enrichment of PC species with 18:1-18:1 took place in all membranes, PC species with 16:0-18:1, 18:0-18:1, 18:1-18:2, 18:1-20:1, and 18:1-22:6 were only enriched in the ER and distal Golgi membranes (not in *cis*/medial Golgi membranes). However, PC species with 14:0-16:0, 16:0-16:1, and 16:0-16:0 were decreased in *cis*/medial Golgi membranes. In the case of PE, nearly all species in the ER membranes were markedly increased, but lesser changes occurred in *cis*/medial and distal Golgi membranes (Table III). In the latter two compartments, PE species containing saturated (16:0 and 18:0), monounsaturated (16:1 and 18:1), and diunsaturated (18:2) acyl chains were markedly reduced by oleate treatment.

The effects of oleate treatment on the PC and PE molecular species within the lumen were also determined. Oleate treatment resulted in increased PC (by 56%) and PE (by 108%) mass in the lumen of total microsomes (Fig. 11, *C* and *D*). Although lipoproteins containing apoB100 was absent in the ER lumen, marked increase in PC and PE mass by oleate treatment was detected here. In fact, lumenal PC and PE mass was increased in all subcellular compartments. For instance, lumen PC (mainly species with 18:1) was increased by 52, 42, and 91% in ER, *cis*/medial Golgi, and distal Golgi, respectively (Fig. 11*C* and Table IV). Similarly, elevation of most PE species occurred in the lumen of all subcellular compartments with the highest increase in the distal Golgi lumen (Fig. 11*D* and Table V). The increased lumenal PC and PE mass cannot be an artifact resulting from membrane rupture by homogenization or carbonate treatment, because the molecular species of PC and PE in the lumen were obviously distinct from those associated with the membranes (Tables II–V). It is possible that the ER lumenal PC and PE are part of the previously reported lipid entities devoid of apoB (27). We also determined molecular species of PC that are associated with secreted lipoproteins. Oleate treatment markedly increased PC species with 18:1 in $VLDL_1$ and $VLDL_2$ had no effect in IDL/LDL and resulted in decrease in HDL (Table VI). Although to a lesser extent, other PC species were also increased in VLDL and decreased in HDL by oleate

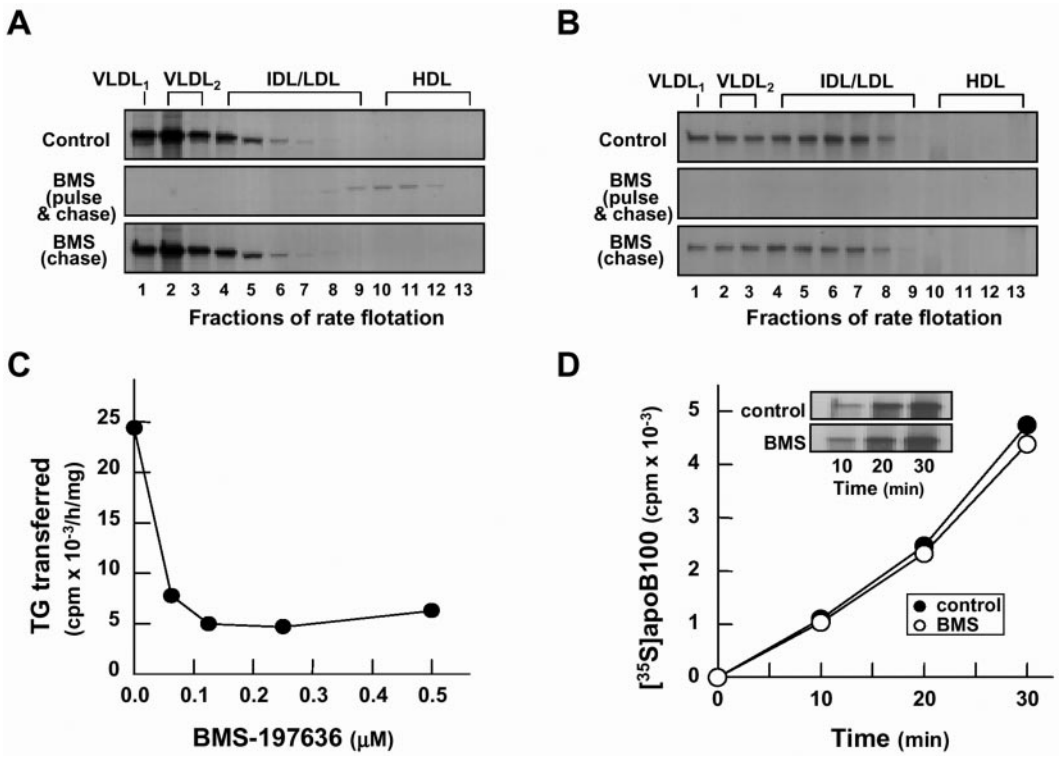

FIG. 10. **MTP activity is not required for the VLDL assembly and secretion after apoB exited ER.** The cells were pretreated with or without 0.2 μM of MTP inhibitor (BMS-197636) for 30 min, pulse-labeled with [^{35}S]methionine/cysteine for 20 min, and chased for 45 min. In one set of experiments, the inhibitor was present throughout pulse and chase (*BMS (pulse & chase)*). In the other set, the inhibitor was added during the last 30 min of chase (*BMS (chase)*). Medium (*A*) and lumenal content of distal Golgi (fractions 1–3) (*B*) were collected and subjected to cumulative rate flotation centrifugation. ^{35}S-apoB100 was immunoprecipitated with anti-human apoB antiserum and resolved in SDS-PAGE/fluorography. *C*, cells were incubated with various concentrations of MTP inhibitor (0–0.5 μM) for 30 min in the presence of 0.4 mM oleate. The cell lysates were subjected to MTP assay. Note that about 80% of MTP was inactivated during 30 min of incubation with the inhibitor. *D*, cells were pretreated with 0.2 μM of BMS-197636 for 30 min and then labeled with [^{35}S]methionine/cysteine for 10, 20, and 30 min in the presence of MTP inhibitor. Oleate (0.4 mM) was present throughout the experiment. The cells were solubilized, and total ^{35}S-apoB100 was immunoprecipitated and detected by SDS-PAGE/fluorography.

treatment. The secreted PE species were not determined because of low abundance. Together, data of lipid analysis revealed that the oleate-induced VLDL assembly and secretion was associated with drastically altered phospholipid content and composition in the membranes of the secretory pathway.

DISCUSSION

The rat hepatoma McA-RH7777 cells retain the ability to synthesize and secrete TG-rich VLDL (*i.e.* $VLDL_1$, $S_f > 100$) when cultured in the presence of exogenous oleate. By transfecting human apoB100 into these cells, we have been able to investigate the biochemical events during assembly of VLDL containing human apoB100 (19). The current study was intended to determine the subcellular compartments where the oleate-induced assembly of apoB100-VLDL (*i.e.* incorporation of bulk TG) was achieved. Using comprehensive biochemical approaches, we have determined the path through which the membrane-bound nascent apoB100 polypeptides are converted into buoyant VLDL. The transition from membrane-bound apoB100 to VLDL occurs clearly as the nascent apoB100 polypeptides move from ER to the distal Golgi (Figs. 3, 5, and 6). In this study, the identities of ER and Golgi microsomes have been authenticated not merely by exhaustive immunolocalization of the marker proteins among the Nycodenz fractions (*e.g.* calnexin, MTP, protein disulfide isomerase, Grp94, Bip, Hsp47, ERGIC53, β-COP, ManII, COPII, and TGN38) (Figs. 1, *A–C*, and 4*D*). In addition, they are validated by the distribution of sphingomyelin with respect to PC (Fig. 4*B*) and by the glycosylation status of human apoB100 at various subcellular compartments (Fig. 7). The demonstration that the appearance of VLDL in the lumen coincided with apoB100 gaining Endo H resistance suggests strongly that assembly of VLDL must be achieved in post-ER compartments in these cells. Thus, the current work, as a sequel of our previous studies showing the temporal features associated with post-translational VLDL formation (2), has provided new insights into the spatial perspectives of apoB100-VLDL assembly in McA-RH7777 cells.

Three observations from the current study are noteworthy. First, the appearance of apoB100-VLDL observed within the distal Golgi lumen occurs almost concurrently with the secretion of apoB100-VLDL into the medium (Fig. 6). This observation provides solid evidence that the compartment where apoB100-VLDL is assembled must be in close proximity to the site for its secretion. Moreover, this observation also indicates that mature apoB100-VLDL particles, once assembled with bulk neutral lipids, are immediately secreted and not retained within the Golgi. The identical glycosylation status of VLDL-associated apoB100 between distal Golgi lumen and medium (Fig. 7, *B* and *C*) indicates the former being direct precursors of the latter. The rapid release of apoB100-VLDL after full assembly is also supported by the pulse-chase data that the amount of ^{35}S-apoB100 in the lumen is 10–20-fold lower than that in the medium during chase. The low abundance of apoB100-VLDL within the microsomal lumen has also been observed in cultured rat hepatocytes (28). Thus, the current results, in agreement with conclusions drawn previously by Bamberger and Lane (4, 17) that VLDL assembly occurs in the Golgi, indicate that apoB100-VLDL has a transient nature within the distal Golgi.

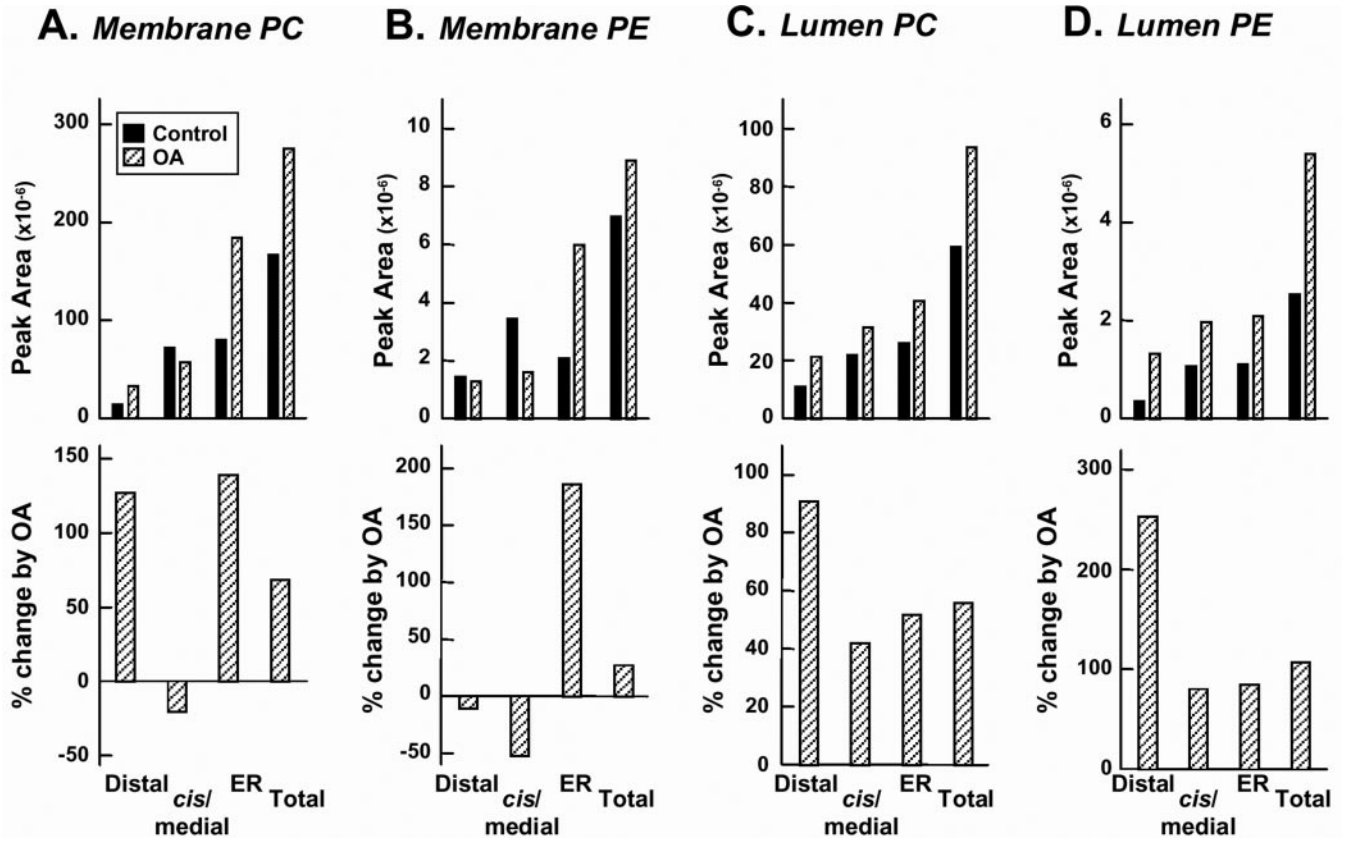

FIG. 11. **Distribution of PC and PE in membranes and lumenal contents of subcellular compartments.** The cells were incubated with (*hatched bars*) or without (*black bars*) 0.4 mM oleate for 18 h. The subcellular compartments were fractionated by the Nycodenz gradient centrifugation, and the membranes and lumenal contents of distal Golgi (fractions 1–3), *cis*/medial Golgi (fractions 4–8), and ER (fractions 9–15) were isolated by sodium carbonate treatment followed by ultracentrifugation. Lipids of the membranes (*A* and *B*) and lumenal contents (*C* and *D*) of subcellular compartments were extracted and subjected to electrospray tandem mass spectrometry for the analysis of PC (*A* and *C*) and PE (*B* and *D*) as described under "Experimental Procedures."

TABLE II
Analysis of membrane PC species

Single underlines indicate species that showed mass increase, and double underlines indicate species that showed mass decrease by treatment with oleate (OA).

Species	Peak Area ($\times 10^{-6}$)					
	Distal Golgi		*cis*/medial Golgi		ER	
	Control	OA	Control	OA	Control	OA
14:0–14:0[a]	0.14	0.14	0.14	0.14	0.14	0.14
14:0–16:0	0.24	0.45	1.56	0.45	0.86	1.00
16:0–16:1	0.80	1.04	5.34	1.87	6.69	5.80
16:0–16:0	0.61	0.94	2.37	1.20	2.12	3.23
16:1–18:2	0	0	0	0	0	0
16:0–18:2	0.82	1.13	4.48	3.11	6.59	10.33
16:0–18:1	2.51	5.33	13.21	9.60	16.44	33.37
16:0–20:5, 18:2–18:3	0.08	0	0.38	0	0.60	0
16:0–20:4, 18:2–18:2	0.13	0	0.63	0	1.04	0
18:1–18:2, 16:0–20:3	0.30	0.47	1.24	0.91	1.90	3.49
18:1–18:1, 18:0–18:2	0.94	4.72	5.32	11.74	7.04	43.25
18:0–18:1	0.83	2.11	3.47	3.74	3.32	12.17
18:0–18:0	0.13	0	0.48	0	0	0
18:2–20:5	0	0	0	0	0	0
16:0–22:6, 18:2–20:4	0.10	0.16	0.35	0.30	0.85	1.05
18:1–20:4, 16:0–22:5, 18:0–20:5	0.09	0.19	0.47	0.59	0.86	1.50
18:0–20:4, 18:1–20:3	0.08	0.17	0.40	0.43	0.72	1.42
18:0–20:3	0.15	0.24	0.51	0.47	0.68	1.58
18:1–20:1	0.47	1.27	1.75	1.59	1.42	4.50
18:2–22:6	0.03	0.05	0.04	0.05	0.04	0.11
18:1–22:6, 18:2–22:5	0.03	0.15	0.32	0.34	0.43	0.82
18:0–22-6, 18:1–22-5	0.14	0.10	0.42	0.10	0.46	0.70

[a] Internal standard.

Second, transit of lipoprotein particles through the Golgi results in a 1.4-fold increase in the average diameter (and a 2.7-fold increase in volume, assuming spherical particles) and a shift from two smaller toward three larger diameter species. These observations are compatible with lipid recruitment across the stacked Golgi. The average diameter (40 nm) of

TABLE III
Analysis of membrane PE species

Single underlines indicate species that showed mass increase, and double underlines indicate species that showed mass decrease by treatment with oleate (OA).

Species	Peak area ($\times 10^{-5}$)					
	Distal Golgi		*cis*/medial Golgi		ER	
	Control	OA	Control	OA	Control	OA
14:0–16:0	0	0	0	0	0	0
16:0–16:1	0.25	0.18	0.92	0.24	0.4	0.60
16:0–16:0[a]	0.31	0.31	0.31	0.31	0.31	0.31
16:1–18:2	0.27	0.20	0.34	0.24	0.26	0.48
16:0–18:2	0.70	0.31	1.43	0.51	1.07	1.47
16:0–18:1	0.76	0.52	2.04	0.38	1.13	2.39
16:0–20:5, 18:2–18:3	0.26	0.13	0.98	0.38	0.40	1.01
16:0–20:4, 18:2–18:2	0.34	0.18	0.52	0.30	0.75	1.31
18:1–18:2, 16:0–20:3	0.55	0.45	1.49	0.34	1.11	2.24
18:1–18:1, 18:0–18:2	1.02	1.10	2.51	1.43	1.17	8.11
18:0–18:1	0.54	0.53	0.58	0.85	0.73	2.49
18:0–18:0	0.20	0.07	0.39	0.10	0.39	0.84
18:2–20:5	0	0	0	0	0	0
16:0–22:6, 18:2–20:4	0.30	0.31	0.84	0.69	1.05	2.19
18:1–20:4, 16:0–22:5, 18:0–20:5	0.57	0.79	0.63	0.83	1.17	4.25
18:0–20:4, 18:1–20:3	0.77	0.86	1.32	0.70	1.34	4.21
18:0–20:3	0.29	0.51	0.33	0.74	0.72	2.19
18:1–20:1	0.28	0.45	0.55	0.31	0.19	0.67
18:2–22:6	0.15	0.24	0.69	0.13	0.33	0.45
18:1–22:6, 18:2–22:5	0.24	0.28	0.32	0.38	0.69	2.21
18:0–22-6, 18:1–22-5	0.77	0.51	1.03	0.63	1.03	2.04

[a]Internal standard.

TABLE IV
Analysis of lumen PC species

Underlines indicate species that showed mass increase by treatment with oleate (OA).

Species	Peak area ($\times 10^{-6}$)					
	Distal Golgi		*cis*/medial Golgi		ER	
	Control	OA	Control	OA	Control	OA
14:0–14:0[a]	0.14	0.14	0.14	0.14	0.14	0.14
14:0–16:0	0.24	0.22	0.4	0.30	0.26	0.26
16:0–16:1	0.68	0.73	1.73	1.00	2.01	1.21
16:0–16:0	0.42	0.60	0.95	0.89	0.80	0.61
16:1–18:2	0	0	0	0	0	0
16:0–18:2	0.53	0.93	1.56	1.33	2.09	2.27
16:0–18:1	1.6	3.43	4.17	5.08	5.37	7.17
16:0–20:5, 18:2–18:3	0.05	0	0.12	0	0.16	0
16:0–20:4, 18:2–18:2	0.09	0	0.19	0	0.25	0
18:1–18:2, 16:0–20:3	0.16	0.34	0.42	0.46	0.54	0.67
18:1–18:1, 18:0–18:2	0.68	3.93	1.61	5.35	2.27	9.45
18:0–18:1	0.68	1.56	1.05	2.20	1.12	3.12
18:0–18:0	0.11	0	0	0	0	0
18:2–20:5	0	0	0	0	0	0
16:0–22:6, 18:2–20:4	0.05	0.10	0.14	0.15	0.22	0.24
18:1–20:4, 16:0–22:5, 18:0–20:5	0.07	0.12	0.13	0.21	0.25	0.33
18:0–20:4, 18:1–20:3	0.06	0.15	0.12	0.25	0.23	0.31
18:0–20:3	0.07	0.18	0.11	0.25	0.23	0.41
18:1–20:1	0.46	0.72	0.46	1.12	0.49	1.00
18:2–22:6	0	0.02	0.03	0.02	0.02	0.01
18:1–22:6, 18:2–22:5	0.05	0.09	0.11	0.12	0.12	0.21
18:0–22-6, 18:1–22-5	0.05	0.10	0.14	0.11	0.16	0.23

[a] Internal standard.

lipoprotein particles in the Golgi of McA-RH7777 cells expressing human apoB100 resembles that of negatively stained lipoproteins, isolated from the lumen of rat liver Golgi fractions (39 nm) (16) or viewed within mouse liver Golgi fractions (35 nm) (18). The five lipoprotein species (~20-, 40-, 50-, 60-, and 75-nm diameter) identified within the Golgi (Fig. 9) cannot be placed in a maturation continuum until the lipid/apolipoprotein content of each species is known. However, isolated HDL-type particles have a maximum diameter of 25 nm, whereas isolated VLDL-type particles range between 30 and 80 nm (29). Thus, the shift from two smaller species in *cis* elements toward the three larger species in *trans* elements is compatible with the biochemical data of assembly of VLDL occurring in the Golgi. The decreases in average lipoprotein particle diameter between saccule 6 and the TGN and between the TGN and the secretory granules are compatible with lipid recruitment ceasing to occur past the stacked Golgi and may reflect remodeling of assembled VLDL.

Third, the newly synthesized apoB100 polypeptides enter the *cis*/medial Golgi compartments as membrane-associated forms that remain Endo H-sensitive. Unlike what was originally thought, that the membrane-associated apoB polypeptides were secretion-incompetent and destined for degradation (30), recent experimental evidence has indicated that the membrane-associated apoBs are the direct precursors of secreted VLDL both in McA-RH7777 cells and in cultured primary rat

TABLE V
Analysis of lumen PE species

Underlines indicate species that showed mass increase by treatment with oleate (OA).

Species	Peak area ($\times 10^{-5}$)					
	Distal Golgi		*cis*/medial Golgi		ER	
	Control	OA	Control	OA	Control	OA
14:0–16:0	0	0	0	0	0	0
16:0–16:1	0.06	0.20	0.10	0.14	0.26	0.32
16:0–16:0[a]	0.31	0.31	0.31	0.31	0.31	0.31
16:1–18:2	0.02	0.06	0.15	0.12	0.05	0.07
16:0–18:2	0.12	0.33	0.62	0.67	0.61	0.67
16:0–18:1	0.20	0.48	0.62	0.87	0.52	0.79
16:0–20:5, 18:2–18:3	0.08	0.30	0.16	0.24	0.34	0.10
16:0–20:4, 18:2–18:2	0.09	0.31	0.18	0.40	0.35	0.38
18:1–18:2, 16:0–20:3	0.11	0.56	0.57	1.00	0.49	0.75
18:1–18:1, 18:0–18:2	0.24	1.55	0.91	2.97	0.98	3.03
18:0–18:1	0.11	0.85	0.29	1.00	0.62	0.90
18:0–18:0	0.06	0.14	0.10	0.10	0.15	0.16
18:2–20:5	0	0	0	0	0	0
16:0–22:6, 18:2–20:4	0.11	0.38	0.60	0.64	0.39	0.61
18:1–20:4, 16:0–22:5, 18:0–20:5	0.17	0.93	0.68	1.31	0.55	1.48
18:0–20:4, 18:1–20:3	0.24	0.83	0.60	1.24	0.53	1.75
18:0–20:3	0.11	0.43	0.38	0.76	0.44	0.77
18:1–20:1	0	0	0	0	0	0
18:2–22:6	0.02	0.05	0.07	0.06	0.09	0.07
18:1–22:6, 18:2–22:5	0.04	0.32	0.14	0.40	0.19	0.55
18:0–22-6, 18:1–22-5	0.15	0.42	0.40	0.64	0.56	0.77

[a]Internal standard.

TABLE VI
PC species associated with secreted lipoproteins

The conditioned media of cells incubated without (Control) or with oleate (OA) were subjected to rate flotation centrifugation followed by lipid extraction and analysis as described under "Experimental Procedures." Single underlines indicate species that showed mass increase, and double underlines indicate species that showed mass decrease by treatment with oleate (OA).

Species	Peak height ($\times 10^{-4}$)									
	$VLDL_1$		$VLDL_2$		IDL		LDL		HDL	
	Control	OA	Control	OA	Control	OA	Control	OA	Control	OA
14:0–16:0	2	3	2	3	3	3	14	13	30	11
16:0–16:1	4	5	7	7	6	6	19	16	64	20
16:0–18:2	3	12	10	12	10	15	48	44	380	160
16:0–18:1	4	21	10	31	25	36	73	79	292	123
16:0–20:4	1	3	1	4	3	6	3	5	84	31
18:1–18:2	2	4	3	6	5	8	14	15	142	53
18:1–18:1	3	29	9	35	25	34	91	90	696	260
18:0–18:1	4	11	7	17	26	32	71	73	253	101
18:0–18:0	2	2	1	3	3	2	14	18	10	2
18:0–20:4	3	3	3	4	6	10	14	13	96	32
18:0–20:3	2	2	2	4	6	12	18	20	70	26
18:1–20:1	2	6	4	8	12	14	29	28	50	18
18:0–22:6	1	2	1	2	2	4	8	5	40	13

hepatocytes (11, 12, 28). Thus, the near absence of apoB100 in the lumen of ER and *cis*/medial Golgi (Figs. 5*B* and 6), the frequent detection by electron microscopy of membrane-associated lipoproteins in the *cis*-, but not *trans*-Golgi (Fig. 8), together with the narrow time window between VLDL assembly and VLDL secretion (Fig. 6) suggested strongly that the secretion-competent VLDL particles utilize membrane-associated apoB100 during assembly. The observed difference in Endo H sensitivity between medium (Endo H-resistant) and membrane-associated apoB100 (Endo H-sensitive) is reminiscent of a previous report that membrane-bound apoB in rat hepatocytes had oligosaccharide moieties distinct from that of apoB in the plasma (31).

Although evidence abounds, the significance of apoB association with membranes during VLDL assembly is unknown, nor is the physical nature of apoB-membrane interactions clear. We have recently postulated that membrane phospholipid remodeling plays an important role in apoB100-VLDL assembly in oleate-treated McA-RH7777 cells (22). In these cells, remodeling of phospholipids is mediated primarily by Ca^{2+}-independent phospholipase A_2 (22). As an attempt to unravel the mechanisms underlying the oleate-induced apoB100-VLDL assembly and secretion, we have quantified PC and PE molecular species in the membranes and lumen of the secretory compartments. Of note was the observation that oleate treatment resulted in increased PC and PE mass in the distal Golgi and ER membranes, respectively, with a concomitant decrease in the *cis*/medial Golgi membranes (Fig. 11, *A* and *B*). In the case of PC, the mass increase was accompanied with noticeable species remodeling: increase in 16:0/18:1, 18:1/18:2, 18:1/20:1, and 18:1/22:6 and decrease in 14:0/16:0, 16:0/16:1, and 16:0/16:0. The importance of this species remodeling is unclear, but it may provide membrane architecture appropriate for intracellular movement of apoB and lipids, the key trafficking events essential for the post-ER VLDL assembly (17). It has been postulated for a while that the physicochemical properties of the intracellular membrane phospholipids are critical to correct sorting and trafficking of proteins (for review see Ref. 32). Changes in membrane phospholipid composition may regulate membrane association and proper folding of apoB100 in

the ER and *cis*/medial Golgi and facilitate acquisition of bulk neutral lipids in distal Golgi. Correct folding of integral membrane proteins by membrane PE (acting as a molecular chaperon) has been reported (33, 34). Alternatively, changes in membrane phospholipid composition may also modulate apoB100 interaction with various molecular chaperons (12, 35) during trafficking and post-ER assembly. Clearly, the purpose of membrane phospholipid remodeling in oleate-induced apoB100-VLDL assembly and secretion merits further study.

Following its movement, the initial apoB100 associated with ER membrane was gradually transferred to the lumen of distal Golgi (Figs. 5 and 6). Although the Endo H-resistant apoB100 associated with various lipoproteins observed within the distal Golgi lumen is suggestive of apoB100-VLDL being assembled here, it by no means rules out the possibility that assembly commences at *cis*/medial Golgi compartments. Although apoB100 was present in ER fractions (Figs. 1, 2, and 7), visible lipoprotein particles were not detectable in ER of McA-RH7777 cells expressing human apoB100, using the same TEM protocol that detected particles as small as 20 nm in diameter in ER of rat primary hepatocytes (data not shown). This may imply that expressed human apoB100 only starts to recruit lipid post-ER. Alternatively, poorly lipidated apoB100 particles are formed in the ER but are too small, diffuse, and/or membrane-embedded to be detected with our current TEM method. Visible lipoprotein particles were first detected in the *cis*-Golgi (Fig. 8), coinciding with the kinetics data showing that *cis*/medial Golgi was the site of apoB100 accumulation during its transit through the secretory pathway (Fig. 3). It is therefore possible that the membrane-bound, Endo H-sensitive apoB100 starts to combine with bulk neutral lipids within *cis*/medial Golgi. However, the fact that only highly buoyant dense apoB100 particles, instead of VLDL, were releasable from *cis*/medial Golgi membrane by treatment with mild detergent and high salt concentrations, together with the frequent detection of lipoprotein particles associated with the membranes of *cis*-Golgi by TEM, suggests a rapid transit of mature VLDL into the distal Golgi. It should be noted that the Nycodenz fractions we considered as distal Golgi (fractions 1–3) are contaminated by endosomes as observed previously by others (36). Immunolocalization has revealed the existence of endosomal markers in addition to *trans*-Golgi network and Golgi-derived anterograde/retrograde vesicles (Fig. 1). However, confocal merging images demonstrate no co-localization of apoB100 and EEA1, which excludes the possibility that the apoB100-VLDL observed in fractions 1–3 is of endosomal origin.

Although the current data indicate that apoB100-VLDL is assembled at the distal end of the secretory pathway, it was reported previously (16) that apoB-containing lipoprotein particles (mainly apoB48) in the lumen of ER and Golgi of rat liver were identical in terms of lipid composition, buoyant density, and size range, which led to the conclusion that ER was the site of VLDL assembly. The difference in conclusions drawn from the current work and previous studies (16) may stem from differences in lipoproteins containing apoB48 *versus* apoB100. The rat hepatocytes synthesize mainly apoB48, whereas our transfected cells express primarily the full-length apoB100. Like what was found with rat hepatocytes (16), we have observed that apoB48 lipoproteins with buoyant densities resembling that of $VLDL_2$ were detectable in the lumen of both ER and Golgi in apoB48-transfected cells.[2] However, the TG-rich $VLDL_1$ containing apoB48 was detected exclusively in the lumen of distal Golgi. Thus, assembly of TG-rich VLDL (*i.e.* $VLDL_1$, $S_f > 100$) containing either apoB100 or apoB48 is likely accomplished at the distal end of the secretory pathway.

In summary, we have examined the temporal and spatial events that comprise a post-translational, post-ER process for the assembly of VLDL containing human apoB100. The process proceeds through membrane-associated nascent apoB100 in the ER and *cis*/medial Golgi to eventual acquisition of bulk neutral lipids in a distal Golgi compartment adjacent to the site of secretion. Our findings provide new evidence supporting that assembly of apoB100-VLDL is achieved through a stepwise process.

Acknowledgments—We are in debt to our collaborators, R. Milne, Y. Marcel, M. G. Farquhar, C. C. Shoulders, and D. Gordon, who provided various antibodies and reagents used for this study. We thank Dr. J. Ngsee for the assistance in confocal microscopy and Parke-Davis Pfizer for funds supporting primary hepatocyte facilities at the University of Ottawa Heart Institute.

[2] K. Tran and Z. Yao, unpublished observation.

REFERENCES

1. Chan, L. (1992) *J. Biol. Chem.* **267,** 25621–25624
2. Wang, Y., Tran, K., and Yao, Z. (1999) *J. Biol. Chem.* **274,** 27793–27800
3. Bostrom, K., Wettesten, M., Boren, J., Bondjers, G., Wiklund, O., and Olofsson, S. O. (1986) *J. Biol. Chem.* **261,** 13800–13806
4. Bamberger, M. J., and Lane, M. D. (1988) *J. Biol. Chem.* **263,** 11868–11878
5. Janero, D. R., and Lane, M. D. (1983) *J. Biol. Chem.* **258,** 14496–14504
6. Higgins, J. A., and Hutson, J. L. (1984) *J. Lipid Res.* **25,** 1295–1305
7. Swift, L. L. (1995) *J. Lipid Res.* **36,** 395–406
8. Cartwright, I. J., and Higgins, J. A. (1995) *Biochem. J.* **310,** 897–907
9. Higgins, J. A. (1988) *FEBS Lett.* **232,** 405–408
10. Gordon, D. A., Jamil, H., Gregg, R. E., Olofsson, S. O., and Boren, J. (1996) *J. Biol. Chem.* **271,** 33047–33053
11. Rustaeus, S., Stillemark, P., Lindberg, K., Gordon, D., and Olofsson, S. O. (1998) *J. Biol. Chem.* **273,** 5196–5203
12. Stillemark, P., Boren, J., Andersson, M., Larsson, T., Rustaeus, S., Karlsson, K. A., and Olofsson, S. O. (2000) *J. Biol. Chem.* **275,** 10506–10513
13. Boren, J., Graham, L., Wettesten, M., Scott, J., White, A., and Olofsson, S. O. (1992) *J. Biol. Chem.* **267,** 9858–9867
14. Boren, J., Rustaeus, S., and Olofsson, S. O. (1994) *J. Biol. Chem.* **269,** 25879–25888
15. Pan, M., Liang, J. J., Fisher, E. A., and Ginsberg, H. N. (2002) *J. Biol. Chem.* **277,** 4413–4421
16. Rusinol, A., Verkade, H., and Vance, J. E. (1993) *J. Biol. Chem.* **268,** 3555–3562
17. Bamberger, M. J., and Lane, M. D. (1990) *Proc. Natl. Acad. Sci. U. S. A.* **87,** 2390–2394
18. Swift, L. L., Valyi-Nagy, K., Rowland, C., and Harris, C. (2001) *J. Lipid Res.* **42,** 218–224
19. McLeod, R. S., Zhao, Y., Selby, S. L., Westerlund, J., and Yao, Z. (1994) *J. Biol. Chem.* **269,** 2852–2862
20. Hammond, C., and Helenius, A. (1994) *J. Cell Biol.* **126,** 41–52
21. Rickwood, D., Ford, T., and Graham, J. (1982) *Anal. Biochem.* **123,** 23–31
22. Tran, K., Wang, Y., DeLong, C. J., Cui, Z., and Yao, Z. (2000) *J. Biol. Chem.* **275,** 25023–25030
23. DeLong, C. J., Shen, Y. J., Thomas, M. J., and Cui, Z. (1999) *J. Biol. Chem.* **274,** 29683–29688
24. Thorne-Tjomsland, G., Dumontier, M., and Jamieson, J. C. (1998) *Anat. Rec.* **250,** 381–396
25. Wetterau, J. R., Aggerbeck, L. P., Bouma, M. E., Eisenberg, C., Munck, A., Hermier, M., Schmitz, J., Gay, G., Rader, D. J., and Gregg, R. E. (1992) *Science* **258,** 999–1001
26. Dahan, S., Ahluwalia, J. P., Wong, L., Posner, B. I., and Bergeron, J. J. (1994) *J. Cell Biol.* **127,** 1859–1869
27. Alexander, C. A., Hamilton, R. L., and Havel, R. J. (1976) *J. Cell Biol.* **69,** 241–263
28. Hebbachi, A. M., and Gibbons, G. F. (2001) *J. Lipid Res.* **42,** 1609–1617
29. Shelness, G. S., and Sellers, J. A. (2001) *Curr. Opin. Lipidol.* **12,** 151–157
30. Cartwright, I. J., Hebbachi, A. M., and Higgins, J. A. (1993) *J. Biol. Chem.* **268,** 20937–20952
31. Wong, L., and Torbati, A. (1994) *Biochemistry* **33,** 1923–1929
32. Sprong, H., van der, S. P., and van Meer, G. (2001) *Nat. Rev. Mol. Cell. Biol.* **2,** 504–513
33. Bogdanov, M., and Dowhan, W. (1998) *EMBO J.* **17,** 5255–5264
34. Bogdanov, M., and Dowhan, W. (1999) *J. Biol. Chem.* **274,** 36827–36830
35. Linnik, K. M., and Herscovitz, H. (1998) *J. Biol. Chem.* **273,** 21368–21373
36. Hamilton, R. L., Moorehouse, A., and Havel, R. J. (1991) *J. Lipid Res.* **32,** 529–543